



P2–P1' macrocyclization of P2 phenylglycine based HCV NS3 protease inhibitors using ring-closing metathesis

Anna Lampa^a, Angelica E. Ehrenberg^b, Aparna Vema^a, Eva Åkerblom^a, Gunnar Lindeberg^a, U. Helena Danielson^b, Anders Karlén^a, Anja Sandström^{a,*}

^a Department of Medicinal Chemistry, Organic Pharmaceutical Chemistry, Uppsala University, BMC, Box 574, SE-751 23 Uppsala, Sweden

^b Department of Biochemistry and Organic Chemistry, Uppsala University, BMC, Box 576, SE-751 23 Uppsala, Sweden

ARTICLE INFO

Article history:

Received 27 April 2011

Revised 21 June 2011

Accepted 22 June 2011

Available online 28 June 2011

Keywords:

HCV

Protease inhibitors

Macrocyclization

Phenylglycine

Metathesis

ABSTRACT

Macrocyclization is a commonly used strategy to preorganize HCV NS3 protease inhibitors in their bioactive conformation. Moreover, macrocyclization generally leads to greater stability and improved pharmacokinetic properties. In HCV NS3 protease inhibitors, it has been shown to be beneficial to include a vinylated phenylglycine in the P2 position in combination with alkenylic P1' substituents. A series of 14-, 15- and 16-membered macrocyclic HCV NS3 protease inhibitors with the linker connecting the P2 phenylglycine and the alkenylic P1' were synthesized by ring-closing metathesis, using both microwave and conventional heating. Besides formation of the expected macrocycles in *cis* and *trans* configuration as major products, both ring-contracted and double-bond migrated isomers were obtained, in particular during formation of the smaller rings (14- and 15-membered rings). All inhibitors had K_i -values in the nanomolar range, but only one inhibitor type was improved by rigidification. The loss in inhibitory effect can be attributed to a disruption of the beneficial π – π interaction between the P2 fragment and H57, which proved to be especially deleterious for the *D*-phenylglycine epimers.

© 2011 Elsevier Ltd. All rights reserved.

1. Introduction

It is estimated that 130–170 million people, or 2.2–3.0% of the world's population are infected by hepatitis C virus (HCV).¹ HCV is a serious health problem that has become the major reason for liver transplantations in the western world.² The standard of care consists of the broad-spectrum antiviral agent ribavirin, in combination with pegylated interferon- α , taken for 24–48 weeks. The treatment is often associated with severe side effects and is only efficient for 45–50% of the patients, depending on the viral genotype.³ Therefore, much effort has been dedicated to the important search for new and more effective therapies, a fact, that is, reflected by the number of drug candidates pending in clinical trials. The expansion of drug-resistant strains of HCV might aggravate anti-HCV therapy and is an issue to consider when developing new drugs.

HCV belongs to the *Flaviviridae* family and contains single stranded (+) RNA. After entry of virus into the host cell, the cytoplasm receives the viral RNA from which a viral polyprotein of 3000 amino acids is synthesized. The polyprotein is further processed into four structural and six non-structural viral proteins.

The structural proteins C, E1, E2 and p7 are needed to build the viral capsid while the non-structural (NS) proteins NS2, NS3, NS4A, NS4B, NS5A, and NS5B are involved in the viral replication machinery.^{4–7}

Of the viral proteins, NS3 is one of the most extensively examined targets for anti-HCV therapy.⁸ NS3 is a dual-activity enzyme of both serine protease and helicase/NTPase activities. In combination with its cofactor NS4A, NS3 is responsible for processing the cleavage between NS3/4A, NS4A/4B, NS4B/5A, and NS5A/5B.⁹ Also, recent data suggest that the NS3 protease interferes with the antiviral defense signaling processes of the infected cell, thereby assisting a more persistent HCV infection.¹⁰ Early studies showed that knock-out of the NS3/4A protease activity by point mutations in an HCV RNA transcript resulted in interruption of viral replication *in vivo*.¹¹ Later, proof of concept was established in humans when administration of the HCV NS3 protease inhibitor BILN-2061 reduced HCV RNA plasma levels significantly, something that has also been established by ensuing inhibitors.¹²

A characteristic of the NS3 protease is that it is inhibited by its N-terminal cleavage product,^{13,14} a property that has been exploited in the development of product-based NS3 protease inhibitors. Such inhibitors possess a C-terminal acidic functionality, typically a carboxylic acid or a bioisostere thereof, for example, an acylsulfonamide (see Fig. 1). Other HCV NS3 protease inhibitors are based on a C-terminal electrophilic group, such as an α -ketoamide, capable of forming a covalent, reversible bond with the catalytic serine.

* Corresponding author. Tel.: +46 18 471 4285; fax: +46 18 471 4474.

E-mail address: Anja.Sandstrom@orgfarm.uu.se (A. Sandström).

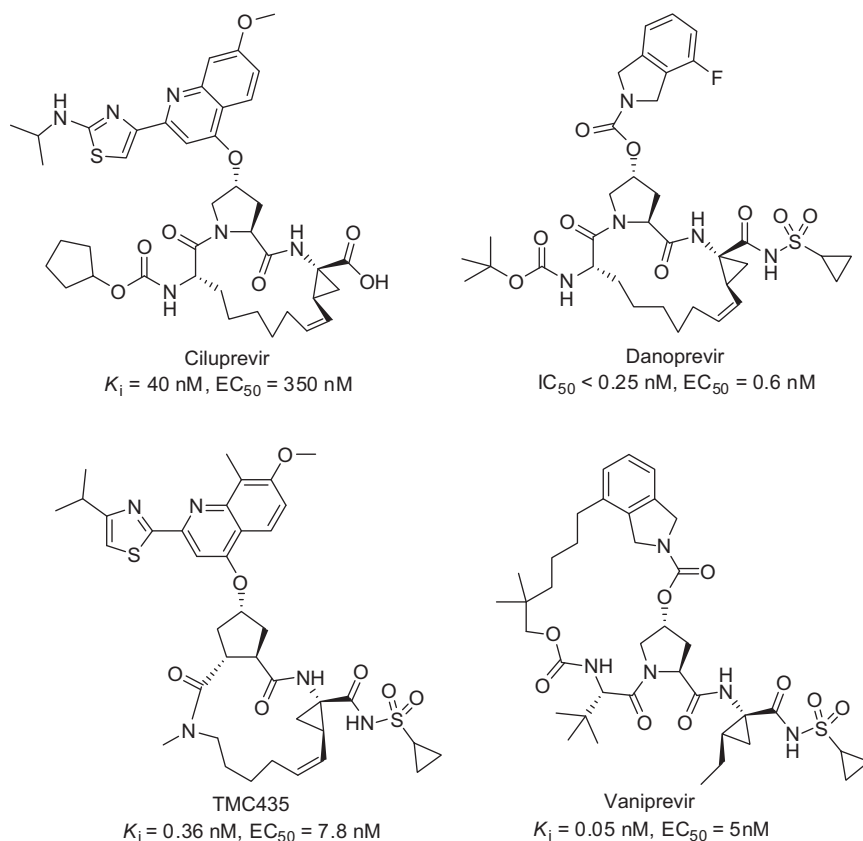


Figure 1. Macrocyclic product-based HCV NS3 protease inhibitors that have been, or are, in clinical trials: Ciluprevir,¹² Danoprevir,^{25,26} TMC435²⁷ and Vaniprevir.^{28,29}

There are currently several HCV NS3 protease inhibitors in different phases of clinical trials. Two of the electrophilic inhibitors, telaprevir (Vertex Pharmaceuticals) and boceprevir (Merck & Co., Inc.), have recently been approved by FDA.^{15,16} Four of the product based inhibitors that have been or are at present, in clinical trials are outlined in Figure 1. Common features are a proline or a proline mimic (TMC435) in the P2 position and a macrocycle linker connecting the P3 and P1 side chains (Ciluprevir, Danoprevir, and TMC435) or connecting the P3 capping group and the P2 substituent (Vaniprevir). Inhibitors based on peptide sequences often suffer from low bioavailability and poor pharmacokinetic properties.¹⁷ Common strategies to overcome these problems involve incorporation of unnatural amino acids,^{18,19} peptide isosteres²⁰ or macrocycles^{21,22} in the peptide sequence. If macrocyclization preorganizes the inhibitor in its bioactive conformation it can interact with the protease with reduced loss of entropy and enhanced binding. Indeed, macrocyclization has proven to be a successful approach for several product based HCV NS3 protease inhibitors.^{23,24}

We have previously reported on phenylglycine (Phg) as an alternative P2 moiety in HCV NS3 protease inhibitors,³⁰ invoking an advantageous resistance profile³¹ and structure–activity relationships different from proline-based inhibitors. Some structural moieties, such as the vinyl-ACCA in P1, that are optimized to suit proline-based inhibitors are rarely beneficial for phenylglycine-based inhibitors. These findings suggest an alternative binding mode for phenylglycine-based inhibitors. For example, phenylglycine might interact with the catalytic H57 by π – π stacking.³⁰ The aromaticity of phenylglycine also allows for chemical modifications that can be used in optimization processes. Both modeling and inhibition experiments suggest that phenylglycine-based inhibitors have the possibility to retain the same conformation when binding to A156T and D168V mutated forms of the protease

as when binding to the wild-type enzyme. In contrast, mutated forms of protease create an imposed change in binding conformation for P2 proline based compounds, and thereby loss of inhibitory potency.³² Yet, an X-ray structure of a phenylglycine-based inhibitor co-crystallized with the enzyme would be required to draw accurate conclusions about the binding conformation. Although phenylglycine-based inhibitors are promising alternatives to the proline-based inhibitors, significant improvements in inhibitory potencies are required.

An optimization strategy previously reported by us³³ includes the introduction of a vinyl in the 3-position of the phenylglycine and an alkenylic P1' elongation (Compounds A, Fig. 2). Especially the alkenylic P1' extensions proved to be beneficial for inhibitory effects of the compounds. However, a positive effect of the vinylic substitution was observed for the inhibitors based on *D*-phenylglycine, which according to modeling could be due to a postulated π – π interaction between H57 and mainly the vinyl in this case (Fig. 2).^{30,33}

Docking further indicated proximity between the alkenylic P1' linker and the P2 position (see Fig. 2), which inspired us to explore the corresponding macrocyclization. Although the vinyl and the P1' side chain are positioned in opposite directions in the model, we were interested in investigating the outcome of a corresponding macrocyclization. To our knowledge, similar types of P2–P1' macrocyclizations have not been explored thoroughly in HCV NS3 protease inhibitors previously, besides that described in a very recent patent application on proline-based inhibitors.³⁴ In addition, we expected that macrocyclization could help in validating the accuracy of the model as well as probing the bioactive conformation of phenylglycine-based inhibitors.

Herein the synthesis and biochemical evaluation of a series of tripeptidic P2 phenylglycine-based HCV NS3 protease inhibitors

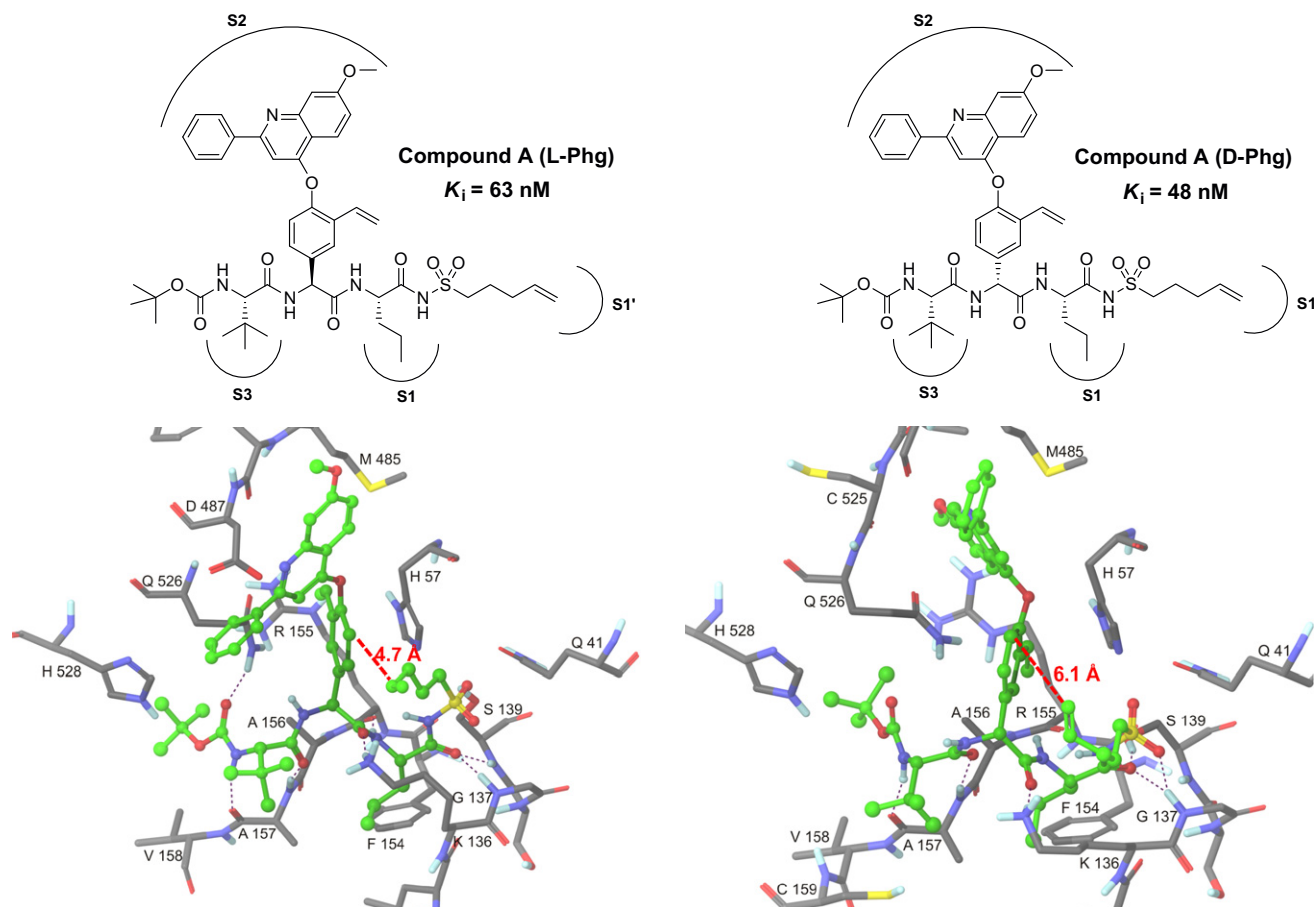


Figure 2. Above: Acyclic P2 phenylglycine-based inhibitors based on L-phenylglycine (to the left) and D-phenylglycine (to the right), with the binding pockets of the protease indicated (S3–S1'). Below: Docked poses of the compounds above in the full length NS3 protease binding site (PDB code: 1CU1). The protease residues are displayed as sticks.³³ A π – π interaction between H57 and the phenyl of the L-phenylglycine (to the left) compound is suggested in the docking solution, whereas the vinyl is proposed to take a larger part in the H57 interaction for the D-phenylglycine compound (to the right). The measured distances in Angstrom between the P1'-linker and the P2 residue are indicated in red (i.e., 4.7 Å and 6.1 Å in the compounds based on L-phenylglycine and D-phenylglycine, respectively).

encompassing a macrocycle spanning P1' and P2 is reported. The macrocyclic inhibitors were synthesized using ring-closing metathesis and include 14–16-membered macrocycles with different aromatic or aliphatic moieties built into the linker. Several products were formed during the metathesis reaction, both ring-contracted and double-bond migrated products. The product pattern was further complicated by the presence of both L- and D-phenylglycine epimers. Although the product picture was very complex, we managed to isolate several potential inhibitors that provided us with a SAR and information about the bioactive conformation.

2. Results

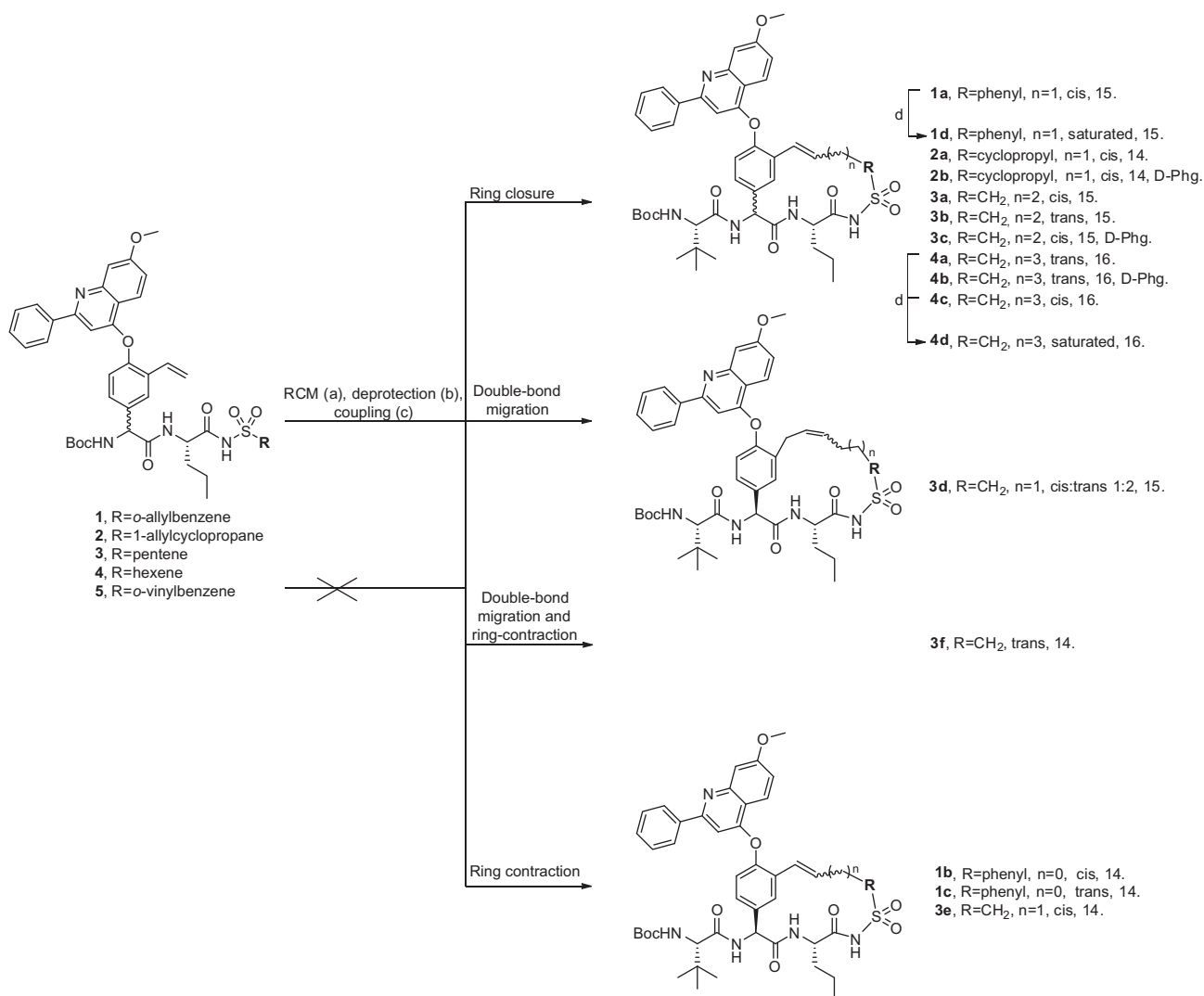
2.1. Chemistry

Dipeptidic compounds **1–5** (Scheme 1), with vinylated phenylglycine and various alkenylic elongations in P1' were all synthesized as described previously. Due to racemization of the phenylglycine during the Suzuki vinylation, compounds **1–5** were mixtures of L-Phg and D-Phg isomers in a 2:1 ratio.³³ Ring-closing metathesis of compounds **1–5** led to the isolated macrocyclic products **1a–d**, **2a–b**, **3a–f** and **4a–d** (Scheme 1). Not all of compounds **1–5** underwent ring-closure by conventional heating in toluene using Grubb's 2nd catalyst at 85 °C, so various ruthenium catalysts, solvents, additives and temperatures were eventually used (vide

infra). It should be emphasized that several isomers were formed during the ring-closure and their isolation was sometimes extremely difficult, a fact that influenced the final yields significantly. Only pure middle fractions were collected and only the inhibitors that could be isolated in pure form were evaluated in the inhibition assay.

Compound **1**, containing an *o*-allyl benzenesulfonamide in the P1' position, was mixed with Grubb's 2nd catalyst and heated in toluene to 85 °C. The starting material was fully consumed only after 40 h of heating and with addition of more catalyst halfway through the reaction. The Boc protecting group was removed using HCl in dioxane and the product subsequently coupled to Boc-L-tLeu using *N*-[(dimethylamino)-1*H*-1,2,3-triazolo-[4,5-*b*]pyridine-1-yl-methylene]-*N*-methylmethanaminium hexafluorophosphate *N*-oxide (HATU) and *N,N*-diisopropylethylamine (DIEA) in DMF. NMR analysis of the purified material revealed that the major product was the expected 15-ring in *cis* configuration (**1a**). In addition, the 14-membered rings **1b** (*cis*) and **1c** (*trans*) were obtained. Reduction of **1a** with PtO₂ in methanol under H₂-atmosphere yielded the saturated compound **1d**.

From compound **2**, with a 1-allylcyclopropane sulfonamide in the P1' position, the desired 14-membered ring was produced in very low yield using the standard conditions. However, microwave-heating at 110 °C for 5 min in trifluorotoluene led to almost full conversion of the starting material. It should be noted that the Boc group remained intact despite the increase in temperature. No



Scheme 1. Reagents and conditions: (a) Grubb's 2nd catalyst/Hoveyda-Grubb's 2nd catalyst, *p*-benzoquinone, toluene/trifluorotoluene/1,2-dichloroethane, 85 °C/110 °C/130 °C, MW (**1** (29%), **2** (37%), **3** (44%), **4** (86%), **5** (0%)); (b) 4.0 M HCl in dioxane (100%); (c) Boc-*L*-Leu, HATU, DIEA, DMF, rt (**1a** (39%), **1b** (4.5%), **1c** (5.9%), **2a** (27%), **2b** (7.8%), **3a** (6.3%), **3b** (3.3%), **3c** (2.8%), **3d** (3.9%), **3e** (3.6%), **3f** (3.8%), **4a** (8.4%), **4b** (4.1%), **4c** (2.5%)); (d) PtO₂, H₂, MeOH (**1d** (50%), **4d** (13.5%)).

ring-contraction was observed in this case. After subsequent HATU mediated coupling with Boc-*L*-Leu, the *L*- and *D*-phenylglycine isomers (**2a** and **2b**, respectively) with *cis* configuration could be isolated by RP-HPLC.

The same microwave method was used on compound **3**, bearing a 4-pentene sulfonamide. After ring-closure followed by coupling with Boc-*L*-Leu several products could be isolated. Thus, both *cis* (**3a**, **3c**) and *trans* (**3b**) products of the expected 15-membered rings, in both the *L*- (**3a** and **3b**) and *D*- (**3c**) phenylglycine configuration were formed. Migration of the double-bond resulted in **3d** (15-ring) in a *cis/trans* ratio of 1:2. Ring-contraction was also observed (**3e**, 14-ring), as well as ring-contraction with double-bond migration (**3f**, 14-ring).

The results above showed that ring-closure of **1**, **2** and **3** required different methods. For example, **2** did not cyclize using conventional heating, while it was almost fully converted using the microwave method. For compound **3** microwave-heating resulted in ring-contraction and double-bond migration besides formation of the expected product. Although the problems with double-bond migration and ring-contraction described above paradoxically led to isolation of several potential inhibitors, we wanted to examine what impact the different methods had on the outcome of the reaction and if the increased temperature and microwave irradiation resulted in

formation of more ring-contracted and double-bond migrated products. Consequently, the ring-closing metathesis reaction of the next compound (**4**), with a 5-hexene sulfonamide, was carried out using three different methods. The reaction products were analyzed by chiral HPLC, LC-MS and NMR. *Method 1*, using Grubb's 2nd catalyst in toluene and conventional heating at 85 °C, was compared to *Method 2*, using Grubb's 2nd catalyst in trifluorotoluene and heating at 110 °C by microwave irradiation, and *Method 3*, using Hoveyda-Grubb's 2nd catalyst in dichloroethane, *p*-benzoquinone, and microwave irradiation at 130 °C. *p*-Benzoquinone has previously been shown to reduce the amount of undesired ring-contracted and double-bond migrated isomers during ring-closing metathesis.³⁵ However, in this case no double-bond migration occurred and contracted rings were formed in only 5–8% of the total conversion yield (Table 1). The presence of *p*-benzoquinone did not reduce the amount of ring-contracted product. It seems, therefore, that the formation of different isomers is more dependent on the substrate. Thus, the expected products (16-membered rings) from the diastereomeric starting material **4** (based on the enantiomeric pair of *L*- and *D*-phenylglycine) are formed in ca. 92–95% yield and the ring-contracted products in a total yield of ca. 5–8%. It might be worth mentioning that the Boc protecting group remained intact in all cases despite which method was used.

Table 1
Products formed using three different methods for ring-closing metathesis of compound **4**

	<i>trans</i> , L-Phg, precursor to 4a	<i>trans</i> , D-Phg, precursor to 4b	<i>cis</i> , L-Phg, precursor to 4c	<i>cis</i> , D-Phg, final product not isolated	Ring contraction
Method 1	58.4%	23.1%	7.7%	5.3%	5.1%
Method 2	54.9%	20.2%	13.6%	4.2%	7.1%
Method 3	51.7%	20.9%	15.1%	4.3%	7.9%

Method 1: Grubb's 2nd catalyst, toluene, 85 °C, 6 h. Method 2: Grubb's 2nd catalyst, trifluorotoluene, MW, 110 °C, 5 min. Method 3: Hoveyda-Grubb's 2nd catalyst, dichloroethane, *p*-benzoquinone, MW, 130 °C, 5 min.

After deprotection of the crude material obtained from ring-closing metathesis of **4** and coupling with Boc-*L*-tLeu the corresponding final products **4a** with *trans* configuration (16-ring, *L*-Phg isomer), **4b** with *trans* configuration (16-ring, *D*-Phg isomer) and **4c** with *cis* configuration (16-ring, *L*-Phg isomer) could be isolated in pure form by preparative chiral HPLC. However, the saturated 16-ring **4d** was obtained by reduction of a mixed fraction of the *L*-phenylglycine isomer products **4a** and **4c**, using PtO₂ in methanol under H₂-atmosphere.

For the cyclization of **5** with an *o*-vinylbenzene sulfonamide aiming at a 14-membered ring, several methods were tried. Heating of **5** with Grubb's 2nd catalyst in toluene 85 °C resulted in very small amounts of desired product (14-ring), a small amount of polymer and mostly starting material remained after 77 h. Change of method, to microwave irradiation at 110 °C for 5 min with Grubb's 2nd catalyst in trifluorotoluene gave the same unsatisfying result, as did change of catalyst to Hoveyda-Grubb's 2nd catalyst and microwave irradiation at 120 °C for 10 min in trifluorotoluene. A last attempt to ring-close compound **5** was made with [1,3-bis(2-methylphenyl)-2-imidazolidinylidene]dichloro-(benzylidene)(tricyclophosphine)ruthenium(II), a catalyst designed for ring-closing metathesis of sterically hindered olefins, heated in trifluorotoluene by microwave irradiation at 130 °C for 1 h. Yet again, no formation of product could be seen. Thereafter, no further attempts in ring-closing **5** were made.

2.2. Biochemical evaluation

K_i-Values for compounds **1a–4d** were determined as described previously³⁶ in an inhibition assay using the full length NS3 protein expressed from mRNA of genotype 1a and a peptide fragment of 16 amino acids corresponding to the activating region of NS4a (Tables 2 and 3). Compounds **1a**, **2a** and **3b** were also evaluated for EC₅₀-values in a replication system using the Huh-7 cell line containing subgenomic HCV RNA genotype 1b replicon with firefly luciferase.³⁷ Only compound **3b** with an EC₅₀-value of 6 μM measured an EC₅₀-value lower than 10 μM.

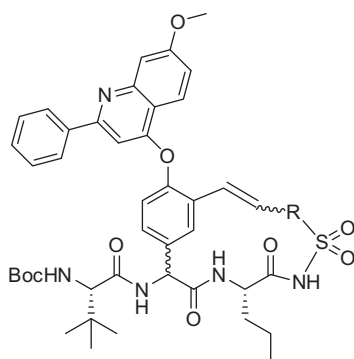
3. Discussion

It has previously been shown that a vinyl moiety on the P2 phenylglycine in combination with alkenylic prime side-substituents improve the activity of P2 phenylglycine-based HCV NS3 protease inhibitors (Fig. 2). The alkenylic P1' substituent seems to reach the space between K136 and Q41, thereby maximizing the hydrophobic contact giving the best inhibitor of this type a K_i-value of

35 nM. Interestingly, the configuration of the phenylglycine has a small impact on the inhibitory effect. Molecular modeling suggests that the vinyl substituent of the *D*-phenylglycine-based inhibitors have a favorable π–π interaction with the catalytic H57 that can compensate for the lost π–π interaction with the aromatic side chain of phenylglycine visualized for the *L*-epimers (Fig. 2).³³

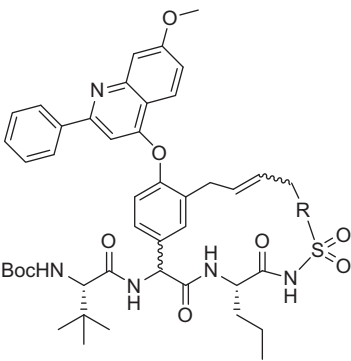
Molecular modeling also inspired us to exploit the proximity of the P1' sulfonamide substituents and the P2 residue to develop macrocyclic HCV NS3 protease inhibitors with a linker connecting the P2 and P1' side chains (Fig. 2). Although the vinyl on the P2 phenylglycine and the alkene substituent in P1' were pointing in opposite directions in the model they could be utilized for cyclization via ring-closing metathesis. We hoped to find compounds with enhanced binding and advantageous pharmacokinetic properties and to gather information about the bioactive conformation, especially the vinyl/phenylglycine interaction with H57, that might strengthen the suggested hypothesis. Thus, phenylglycine-based P2-P1' macrocyclic HCV NS3 protease inhibitors of different ring-sizes (14–16 atoms) and with various sulfonamide linkers were synthesized using ring-closing metathesis (Scheme 1 and Tables 2 and 3). Based on the distance between the two connection points in the model (Fig. 2) and docking of compounds of different ring sizes (e.g., Fig. 3, vide infra), while considering both ring strain and bulkiness, 14–16-membered rings appeared as reasonable candidates for this initial study. Besides the target substances, some side-products caused by ring-contraction and/or double-bond isomerization could be isolated and evaluated as inhibitors.



Ring-closure of compound **2** was not possible under conventional metathesis conditions (toluene, Grubbs 2nd catalyst, 85 °C). However, running the reaction in trifluorotoluene in a microwave synthesizer yielded macrocyclic products in only 5 min. This rapid method was then applied for cyclization of compound **3**. Since small amounts of macrocyclic byproducts were formed by ring-contraction and double-bond migration, a phenomenon that have been observed earlier for ring-closing metathesis,^{38–40} we wanted to examine what impact different metathesis methods had on the ring-closure of **4**. The standard method using Grubb's 2nd catalyst and conventional heating was compared with microwave-heating under similar conditions and also with microwave-heating using Hoveyda-Grubb's 2nd catalyst in the presence of *p*-benzoquinone, a ruthenium hydride scavenger that has proven successful in suppressing double-bond migration in other cases.³⁵ However, it turned out that in the cyclization of **4** only the expected products and small amounts of ring-contracted products (5–8%) were formed regardless of the method used. No method was successful in ring-closing the *o*-vinylbenzene sulfon-

Table 2Cyclized inhibitors. Enzyme inhibition constants (K_i -values) measured with wild-type full-length NS3, genotype 1a

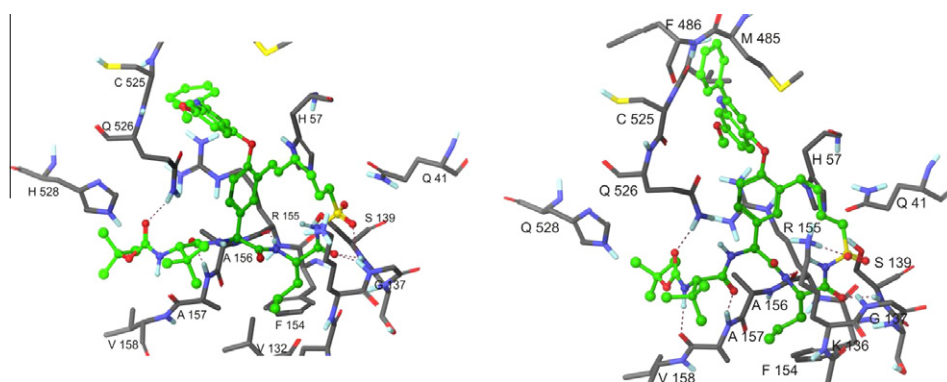
Compound	R	Ring size	Double-bond configuration	Phg configuration	$K_i \pm \text{SD}$ (nM)
1a		15	<i>cis</i>	L	190 ± 50
1b		14	<i>cis</i>	L	170 ± 40
1c		14	<i>trans</i>	L	150 ± 40
1d		15	Saturated	L	250 ± 40
2a		14	<i>cis</i>	L	110 ± 18
2b		14	<i>cis</i>	D	870 ± 110
3a		15	<i>cis</i>	L	390 ± 25
3b		15	<i>trans</i>	L	240 ± 22
3c		15	<i>cis</i>	D	760 ± 100
3e		14	<i>cis</i>	L	137 ± 18
4a		16	<i>trans</i>	L	940 ± 120
4b		16	<i>trans</i>	D	710 ± 70
4c		16	<i>cis</i>	L	320 ± 40
4d		16	Saturated	L	570 ± 75

SD, standard deviation.

Table 3Cyclized, double-bond migrated, inhibitors. Enzyme inhibition constants (K_i -values) measured on wild-type enzyme, genotype 1a


Compound	R	Ring size	Double-bond configuration	Phg configuration	$K_i \pm \text{SD}$ (nM)
3d		15	<i>cis:trans</i> 1:2	L	470 \pm 50
3f		14	<i>trans</i>	L	222 \pm 24

SD, standard deviation.

**Figure 3.** Compound **4a** (green, left) and compound **3e** (green, right) docked in the full-length NS3 protease binding site (PDB code: 1CU1). The protease residues are displayed as sticks.

amide compound **5** to yield the 14-membered ring with an aryl-containing linker. Interestingly, a 14-membered ring could be obtained as a ring-contracted byproduct from the cyclization of the *o*-allylbenzenesulfonamide analog **1**, forming compounds **1b** and **1c**.

Taken together, despite the similarities of substrates **1**, **2**, **3**, **4** and **5** they required different conditions and yielded different outcomes upon macrocyclization. Formation of the 14-membered macrocycles needed increased temperature, and microwave irradiation for substrate **2** and was not possible for substrate **5**. A possible explanation to the disability of **5** to undergo ring-closing metathesis might be interference with formation of a metallacyclobutane complex of the styrene which then chelates to the sulfonyl oxygen.^{41,42} The 15-membered macrocycles could be formed under conventional heating but formed some ring-contracted (substrates **1** and **3**) and double-bond migrated products (substrate **3**). Formation of the 16-membered macrocycles was uncomplicated and resulted in product formation with only minor amounts of ring-contracted products irrespective of what method was used. This indicates that the outcome of the reaction depends more on the substrate used than the method.

All inhibitors in the macrocyclic series had K_i -values in the upper nanomolar range, with the best inhibitor possessing a K_i -value of 110 nM. All macrocyclic inhibitors except **2a** had lower

inhibitory effect than their acyclic counterparts.³³ A slight preference was seen for the 14-membered macrocycles (compounds **1b**, **1c**, **2a**, and **3e**) over 15- (compounds **1a**, **d** and **3a–d**) and 16-membered macrocycles (compounds **4a**, **4b**, **4c**, and **4d**). Among the 14-membered macrocycles the linker type did not have a large impact on the inhibitory effect. Compound **1b** (K_i = 170 nM) with an aryl linker was slightly less potent than compound **3e** (K_i = 137 nM) with an alkyl linker and compound **2a** (K_i = 110 nM) with a cyclopropyl linker. Comparing the 14-membered macrocycles with aryl linkers in *cis* configuration (**1b**, K_i = 170 nM) and *trans* configuration (**1c**, K_i = 150 nM) reveals that the double-bond configuration is insignificant for the magnitude of the inhibitory effect. Neither does double-bond conjugation with the phenylglycine show any large impact on inhibitory effect (compare conjugated compound **3e**, K_i = 137 nM, with non conjugated compound **3f**, K_i = 222 nM). However, the phenylglycine configuration has a significant influence on the K_i -value. The comparison of the 14-membered macrocycle compounds with cyclopropyl linkers shows an eight-fold preference for the L-configuration (L-isomer **2a**, K_i = 110 nM vs D-isomer **2b**, K_i = 870 nM). This result supports the view that the vinyl has an important π – π interaction with H57, disrupted upon macrocyclization. Notably, the cyclopropyl moiety which is a commonly employed P1' substituent in HCV NS3 protease inhibitors (see Fig. 1) is present in the best inhibitor of this

series (**2a**). In the acyclic series, on the other hand, the cyclopropyl containing inhibitors were the least potent.³³

As was the case for the 14-membered macrocycles, the nature of the different linkers had little impact on the inhibitory activity of the 15-membered macrocycles. Moreover, the inhibitory potency is not much affected by double-bond configuration or saturation of the double-bond. The phenylglycine configuration shows the largest influence on the inhibitory effect also in this case. Again, the L-isomer **3a** ($K_i = 390$ nM) is more potent than the D-isomer **3c** ($K_i = 760$ nM). Interestingly, for the 16-membered macrocycles with straight alkyl linkers, which generally were found to be less efficient inhibitors, the double-bond configuration is of importance. Comparison of the *trans* compound **4a** ($K_i = 940$ nM) and the *cis*-isomer **4c** ($K_i = 320$ nM), shows a threefold preference for the *cis* configuration. These results imply that a conjugated double-bond pointing out from the phenylglycine in a *trans* fashion is not accommodated by the protease for the 16-membered macrocycles, a view, that is, supported by modeling of the 16-membered *trans* inhibitor **4a**. From modeling of the 14-membered *cis* inhibitor **3e** ($K_i = 137$ nM) it seems that the shorter linker tightens the macrocycle and takes up less space. This can explain why the 16-membered macrocycle with *cis* conformation (**4c**) is preferred over the *trans* compound (**4a**).

To summarize, our previous assumption that π – π stacking between H57 and the P2 phenyl (in the acyclic L-isomers) or the P2 vinyl (in the acyclic D-isomers) is of importance is strengthened in this study. Although all the macrocyclic inhibitors possess K_i -values in the nanomolar range, they are generally less potent than their acyclic precursors.³³ Thus, it seems that upon macrocyclization, the P2 phenyl is forced to twist out of its binding mode perpendicular to the backbone, parallel to H57 into a conformation more parallel to the backbone. Thereby, the beneficial interactions are disrupted.

The inhibitory effects of the macrocyclic D-isomers are 4–16 times lower than for their acyclic counterparts. For the L-isomers the reduction is less pronounced (0.25–9 times). The 14-membered macrocycle incorporating a cyclopropyl linker is, in fact, more potent than its linear precursor. These results support our view that the H57-vinyl interaction, which might be lost in a macrocyclic inhibitor, is more important for the D-isomers. It could be expected that a larger, more flexible linker would allow the vinyl phenylglycine-based compounds to regain the stacking interaction with H57. However, for the 16-membered macrocycles other factors, such as the bulk accompanied by the linker seem to be the limitation.

4. Conclusion

Ring-closing metathesis was used to synthesize tripeptidic P2 phenylglycine-based HCV NS3 protease inhibitors with a macrocycle spanning the P2 and P1' residues. Inhibitors of varying ring size and different linkers were evaluated. Even though the different starting materials are similar, they require different modes of heating for ring-closure. During the ring-closing metathesis, side reactions leading to ring-contraction and double-bond migration were observed and seemed to depend on substrate structure rather than cyclization method. The ring closed inhibitors generally had lower potency than their acyclic counterparts, indicating that the beneficial interactions with H57 were disrupted upon macrocyclization, especially for the D-phenylglycine epimers.

5. Experimental section

5.1. Chemistry

Reagents and solvents were obtained commercially and used without further purification. Thin layer chromatography (TLC) was

performed on aluminium sheets precoated with silica gel 60 F₂₅₄ (0.2 mm). Chromatographic spots were visualized using UV-detection and/or 2% ninhydrin in ethanol solution followed by heating. Column chromatography was performed using silica gel 60 (40–63 μ m). Analytical HPLC–MS was performed on a Gilson-Finnigan ThermoQuest AQA system equipped with a C18 (Onyx Monolithic C18 (50 \times 4.6 mm)) or a C4 (Hichrom ACE C4 (5 μ m, 50 \times 4.6 mm)) column using MeCN/H₂O (0.05% HCOOH) or MeOH/H₂O (0.05% HCOOH) with UV (254 nm) and MS (ESI) detection or on a Gilson Thermo-Finnigan Surveyor MSQ system using MeCN/H₂O (0.05% HCOOH) with ELSD detection, or on a manual system equipped with a C8 (Zorbax SB-C8 (4.8 \times 50 mm)) column using UV (220 or 230 nm) detection. Preparative HPLC–MS was performed on a Gilson-Finnigan ThermoQuest AQA system equipped with a C8 (Zorbax SB-C8 (5 μ m, 150 \times 21.2 mm)) column using MeCN/H₂O (0.05% HCOOH) as the mobile phase with UV (254 nm) and MS (ESI) detection or a manual system equipped with a C8 (Zorbax SB-C8 (21.2 \times 150 mm)) column using UV (220 or 230 nm) detection and MeCN/H₂O (0.05% HCOOH) or MeCN/H₂O (0.09% TFA) or MeCN/H₂O with 25 mM NH₄OAc, pH 6.3 as the mobile phase. Chiral analysis and separation was performed on a HPLC system equipped with a Reprosil CHIRAL-NR-R (250 \times 4.6 mm, 8 μ m) column or a Reprosil CHIRAL-NR-R (250 \times 20 mm, 8 μ m). Purity determinations were done by RP-HPLC using the following conditions (UV detection at 254 nm): System 1 (Onyx Monolithic C18, 50 \times 4.6 mm, MeCN/H₂O with 0.05% HCOOH) and system 2 (Hichrom ACE C4, 5 μ m 50 \times 4.6 mm, MeCN/H₂O with 0.05% HCOOH). Microwave reactions were carried out in a SmithSynthesizer™ or in an Initiator™ single-mode microwave cavity producing controlled irradiation at 2450 MHz. NMR spectra were recorded on a Varian Mercury plus spectrometer (¹H at 399.8 MHz, ¹³C at 100.5 MHz) at ambient temperature. Chemical shifts (δ) are reported in ppm, indirectly referenced to tetramethylsilane (TMS) via the solvent signal (¹H: CHCl₃ δ 7.26, CD₂HOD δ 3.31; ¹³C: CDCl₃ δ 77.16, CD₃OD δ 49.00). Exact molecular masses were determined on Micromass Q-ToF2 mass spectrometer equipped with an electrospray ion source.

5.2. General procedure for synthesis of compounds 1a–c, 2a–b, 3a–e and 4a–d

The acyclic starting materials **1–4** were subjected to ring-closing metathesis as described in detail below. The Boc protecting group was removed by treating the crude cyclized product with 4.0 M HCl in 1,4-dioxane (10 ml/mmol), until the starting material could no longer be visualized by LC–MS. The HCl salt recovered after evaporation of the solvent was used in the ensuing coupling without further purification. The hydrochloride was mixed with Boc-*t*-Leu, HATU, DIEA and DMF and stirred until the starting material disappeared (LC–MS). After addition of ethyl acetate, the organic phase was washed with 0.1 M sodium acetate, pH 4, and evaporated. Purification and separation of isomers was accomplished by preparative HPLC (sometimes repeatedly). Yields of purified final products are calculated from the amount of crude cyclized starting material.

5.2.1. Compounds 1a, 1b and 1c

Compound **1** (65.3 mg, 0.081 mmol) and Grubb's 2nd catalyst (9.30 mg, 0.011 mmol) was heated in dry toluene at 85 °C. After 6 h, more catalyst (7.90 mg, 0.009 mmol) was added. After 20 h of heating, a third portion of catalyst (6.00 mg, 0.007 mmol) was added and the reaction heated for another 20 h. The solvent was evaporated and the crude product purified on silica gel (CH₂Cl₂–MeOH 93:7). After N-deprotection, the cyclic material (18.0 mg, 0.0232 mmol) was coupled with Boc-*t*-Leu (10.7 mg, 0.0463 mmol), HATU (21.2 mg, 0.0557 mmol), and DIEA (30.9 μ L, 0.181 mmol) in

DMF (1.6 ml). Three consecutive purifications by preparative HPLC (MeCN/H₂O (0.1% TFA)) yielded **1a** (8.1 mg, 39%), **1b** (0.92 mg, 4.5%) and **1c** (1.2 mg, 5.9%) as white solids. In a separate experiment, after extensive purification of the crude ring-closed product from **1**, the *cis* and *trans* configurations of the precursors to **1b** and **1c**, could be established by NMR analysis, although the assignment was not possible in the final products. Compound **1a**: ¹H NMR (CD₃OD (TFA salt)): δ 8.59 (d, *J* = 9.3 Hz, 1H), 8.09 (dd, *J* = 1.6, 7.9 Hz, 1H), 7.74–7.70 (m, 2H), 7.68–7.55 (m, 6H), 7.42–7.38 (m, 2H), 7.33 (m, 1H), 7.29 (d, *J* = 7.7 Hz, 1H), 6.83 (d, *J* = 11.4 Hz, 1H), 6.75 (s, 1H), 6.06 (ddd, *J* = 7.9, 7.9, 11.5 Hz, 1H), 5.45 (s, 1H), 4.32–4.23 (m, 2H), 4.15 (m, 1H), 4.11 (s, 3H), 3.95 (s, 1H), 1.75–1.54 (m, 2H), 1.44–1.39 (m, 2H), 1.42 (s, 9H), 0.97 (s, 9H), 0.95 (t, *J* = 7.4 Hz, 3H). ¹³C NMR (CD₃OD (TFA salt)): δ 172.9, 172.3, 172.0, 168.4, 166.7, 158.7, 157.8, 151.6, 145.3, 140.0, 138.9, 137.5, 135.1, 133.7, 133.5, 132.8, 132.2, 131.6, 131.3, 130.8, 130.8, 129.9, 129.7, 127.8, 126.8, 125.8, 123.2, 122.4, 115.5, 102.8, 101.6, 80.6, 63.5, 57.7, 57.0, 55.7, 35.4, 33.8, 31.5, 28.7, 27.1, 20.0, 14.0. HRMS calcd for C₄₉H₅₅N₅O₉S [M+H]⁺ 890.3799, found: 890.3807. HPLC purity (system 1: 93%, system 2: 96%). Compound **1b**: ¹H NMR (CD₃OD (TFA salt)): δ 8.56 (d, *J* = 9.2 Hz, 1H), 8.09–8.05 (m, 2H), 7.91 (m, 1H), 7.79 (dd, *J* = 1.6, 7.2 Hz, 2H), 7.73 (d, *J* = 7.7 Hz, 1H), 7.61–7.54 (m, 5H), 7.52–7.43 (m, 2H), 7.41–7.31 (m, 3H), 6.77 (s, 1H), 5.92 (s, 1H), 4.60 (m, 1H), 4.07 (s, 3H), 4.05 (s, 1H), 1.84 (m, 1H), 1.73 (m, 1H), 1.54–1.47 (m, 2H), 1.45 (s, 9H), 1.04 (s, 9H), 0.98 (t, *J* = 7.3 Hz, 3H). HRMS calcd for C₄₈H₅₃N₅O₉S [M+H]⁺ 876.3642, found: 876.3637. HPLC purity (system 1: 91%, system 2: 95%). Compound **1c**: ¹H NMR (CD₃OD (TFA salt)): δ 8.60 (d, *J* = 9.2 Hz, 1H), 8.10–8.05 (m, 2H), 7.82–7.78 (m, 3H), 7.66–7.49 (m, 8H), 7.47–7.36 (m, 3H), 6.76 (s, 1H), 5.91 (s, 1H), 4.67 (m, 1H), 4.08 (s, 3H), 4.02 (s, 1H), 1.84 (m, 1H), 1.73 (m, 1H), 1.54–1.47 (m, 2H), 1.45 (s, 9H), 1.03 (s, 9H), 0.99 (t, *J* = 7.3 Hz, 3H). HRMS calcd for C₄₈H₅₃N₅O₉S [M+H]⁺ 876.3642, found: 876.3634. HPLC purity (system 1: 99%, system 2: 75%).

5.2.2. Compound 1d

Compound **1a** (4.98 mg, 0.00560 mmol) and PtO₂ (0.75 mg, 0.00330 mmol) were stirred in methanol (2 mL) under H₂-pressure. More PtO₂ (0.75 mg, 0.00330 mmol) was added after 4 hours. The solution was filtered and evaporated after 23 h. Purification by preparative HPLC (MeCN/H₂O (0.1% TFA)) yielded **1d** (2.8 mg, 50%) as a white solid. ¹H NMR (CD₃OD (TFA salt)): δ 8.54 (d, *J* = 9.4 Hz, 1H), 8.04 (dd, *J* = 1.4, 8.1 Hz, 1H), 7.91–7.87 (m, 2H), 7.70–7.56 (m, 7H), 7.54 (dd, *J* = 2.4, 9.3 Hz, 1H), 7.48 (d, *J* = 7.8 Hz, 1H), 7.43–7.30 (m, 2H), 7.20 (s, 1H), 5.49 (s, 1H), 4.34 (dd, *J* = 5.4, 9.2 Hz, 1H), 4.09 (s, 3H), 4.01 (s, 1H), 3.07 (m, 1H), 2.96–2.74 (m, 3H), 2.07–1.94 (m, 2H), 1.86–1.74 (m, 1H), 1.60 (m, 1H), 1.44–1.38 (m, 2H), 1.41 (s, 9H), 1.01 (s, 9H), 0.94 (t, *J* = 7.3 Hz, 3H). ¹³C NMR (CD₃OD (TFA salt)): δ 173.1, 172.5, 171.5, 168.2, 166.6, 158.8, 157.8, 152.8, 142.8, 138.0, 136.7, 135.3, 135.2, 133.9, 133.5, 132.4, 132.3, 131.9, 130.6, 129.8, 129.7, 129.6, 127.4, 125.8, 122.7, 122.4, 115.9, 103.4, 101.5, 80.6, 63.5, 58.1, 57.0, 55.0, 35.4, 33.6, 32.0, 30.4, 29.7, 28.7, 27.1, 19.9, 13.8. HRMS calcd for C₄₉H₅₇N₅O₉S [M+H]⁺ 892.3955, found: 892.3969. HPLC purity (system 1: 95%, system 2: 98%).

5.2.3. Compounds 2a and 2b

Compound **2** (54.5 mg, 0.0708 mmol) was mixed with Grubb's 2nd catalyst (15.8 mg, 0.0403 mmol) and dry trifluorotoluene (23 mL) in a microwave vial and heated by microwave irradiation at 110 °C for 5 min. After filtration, the solvent was evaporated. The crude product was purified on silica (CH₂Cl₂–MeOH 95:5). After N-deprotection, the cyclic intermediate (19.3 mg, 0.0261 mmol) was coupled with Boc-*t*-Leu (12.1 mg, 0.0521 mmol), HATU (23.8 mg, 0.0626 mmol), and DIEA (34.8 μL, 0.204 mmol) in DMF (1 mL). By purification using preparative HPLC (MeCN/H₂O with

25 mM NH₄OAc, pH 6.3) two isomers, **2a** (6.1 mg, 27%) and **2b** (1.5 mg, 7.8%), could be isolated as white solids. For solubility reasons, the products were later transformed to TFA-salts. Compound **2a**: ¹H NMR (CD₃OD (TFA salt)): δ 8.55 (d, *J* = 9.2 Hz, 1H), 7.92–7.89 (m, 2H), 7.68 (d, *J* = 7.6 Hz, 1H), 7.65 (s, 1H), 7.63–7.56 (m, 5H), 7.43 (d, *J* = 8.3 Hz, 1H), 6.81 (s, 1H), 6.61 (d, *J* = 11.6 Hz, 1H), 5.55 (s, 1H), 5.48 (ddd, *J* = 7.4, 8.7, 11.6 Hz, 1H), 4.43 (t, *J* = 7.7 Hz, 1H), 4.11 (s, 1H), 3.98 (s, 1H), 3.19–3.11 (m, 1H), 2.92 (dd, *J* = 7.4, 14.3 Hz, 1H), 1.77–1.57 (m, 2H), 1.48–1.22 (m, 4H), 1.43 (s, 9H), 1.00 (s, 9H), 0.99 (t, *J* = 7.5 Hz, 3H), 0.93–0.86 (m, 2H). ¹³C NMR (CD₃OD (TFA salt)): δ 173.2, 172.9, 172.0, 169.0, 167.1, 158.2, 157.8, 151.4, 144.3, 138.0, 134.0, 132.7, 132.5, 131.4, 130.9, 130.8, 129.9, 129.8, 128.5, 126.0, 123.2, 122.7, 115.4, 102.9, 100.8, 80.7, 63.6, 57.2, 57.1, 55.2, 41.9, 33.4, 28.7, 27.5, 27.1, 20.0, 14.0, 10.8, 8.7. HRMS calcd for C₄₆H₅₅N₅O₉S [M+H]⁺ 854.3799, found: 854.3790. HPLC purity (system 1: 97%, system 2: 89%). Compound **2b**: ¹H NMR (CD₃OD (TFA salt)): δ 8.57 (d, *J* = 10.0 Hz, 1H), 7.83–7.79 (m, 2H), 7.72 (m, 1H), 7.68–7.62 (m, 2H), 7.61–7.56 (m, 4H), 7.46 (d, *J* = 8.9 Hz, 1H), 6.85 (s, 1H), 6.53 (d, *J* = 11.9 Hz, 1H), 5.62 (s, 1H), 5.56 (ddd, *J* = 5.5, 10.3, 11.9 Hz, 1H), 4.40 (t, *J* = 7.8, 1H), 4.11 (s, 3H), 3.78 (s, 1H), 3.22 (m, 1H), 2.51 (m, 1H), 1.95–1.84 (m, 2H), 1.65 (m, 1H), 1.55–1.36 (m, 3H), 1.48 (s, 9H), 1.04–0.99 (m, 2H), 1.00 (s, 9H), 0.98 (t, *J* = 7.2 Hz, 3H). HRMS calcd for C₄₆H₅₅N₅O₉S [M+H]⁺ 854.3799, found: 854.3793. HPLC purity (system 1: 96%, system 2: 97%).

5.2.4. Compounds 3a, 3b, 3c, 3d, 3e and 3f

Compound **3** (105 mg, 0.139 mmol), Grubb's 2nd catalyst (30.0 mg, 0.0353 mmol) and trifluorotoluene was heated by microwave irradiation at 110 °C for 5 min. After filtration of the reaction mixture, the solvent was evaporated. The crude product was purified on silica (CH₂Cl₂–EtOH(95:4)). The material obtained after N-deprotection (42.5 mg, 0.0606 mmol) was coupled with Boc-*t*-Leu (28.0 mg, 0.121 mmol), HATU (55.2 mg, 0.145 mmol), and DIEA (80.8 μL, 0.473 mmol) in DMF (2 mL). Purification by preparative HPLC (MeCN/H₂O with 25 mM NH₄OAc, pH 6.3) yielded **3a** (3.66 mg, 6.3%), **3d** (2.26 mg, 3.9%), **3f** (1.95 mg, 3.8%) as white solids. Compounds **3a** and **3d** were transformed to TFA salts for solubility reasons. By further purification using preparative HPLC (MeCN/H₂O (0.05% HCOOH)) compounds **3b** (1.92 mg, 3.3%), **3c** (1.42 mg, 2.8%) and **3e** (1.80 mg, 3.6%) were recovered as white solids. Compound **3b** was transformed to TFA salt to improve solubility. Compound **3a**: ¹H NMR (CD₃OD (TFA salt)): δ 8.56 (d, *J* = 9.1 Hz, 1H), 7.81 (dd, *J* = 1.7, 7.0 Hz, 2H), 7.69 (d, *J* = 7.3 Hz, 1H), 7.66–7.56 (m, 5H), 7.54 (d, *J* = 2.0, 1H), 7.43 (d, *J* = 8.6 Hz, 1H), 6.81 (s, 1H), 6.45 (d, *J* = 11.4 Hz, 1H), 5.68 (ddd, *J* = 6.9, 7.9, 11.4 Hz, 1H), 5.59 (s, 1H), 4.47 (dd, *J* = 6.7, 8.4 Hz, 1H), 4.11 (s, 3H), 3.97 (s, 1H), 3.33–3.12 (m, 2H), 2.29–2.22 (m, 2H), 1.85–1.60 (m, 4H), 1.43 (s, 9H), 1.49–1.35 (m, 2H), 1.00 (s, 9H), 0.98 (t, *J* = 7.3 Hz, 3H). ¹³C NMR (CD₃OD (TFA salt)): δ 173.8, 173.0, 171.9, 169.0, 167.1, 158.2, 157.8, 151.0, 144.2, 137.9, 136.1, 134.0, 132.8, 131.8, 131.5, 131.3, 131.0, 129.7, 126.1, 124.5, 123.1, 122.7, 115.4, 102.9, 100.7, 80.7, 63.6, 57.2, 57.1, 54.8, 53.3, 35.4, 34.4, 28.7, 28.4, 27.1, 24.9, 20.0, 13.9. HRMS calcd for C₄₅H₅₅N₅O₉S [M+H]⁺ 842.3779, found: 842.3772. HPLC purity (system 1: 95%, system 2: 98%). Compound **3b**: ¹H NMR (CD₃OD (TFA salt)): δ 8.61 (d, *J* = 10.1 Hz, 1H), 7.85–7.81 (m, 2H), 7.73–7.58 (m, 5H), 7.56 (dd, *J* = 2.4, 8.4 Hz, 1H), 7.40 (s, 1H), 7.34 (d, *J* = 8.4 Hz, 1H), 6.76 (s, 1H), 6.44 (d, *J* = 15.7 Hz, 1H), 6.21–6.09 (m, 1H), 5.81 (s, 1H), 4.80 (m, 1H), 4.11 (s, 3H), 3.98 (s, 1H), 3.68 (m, 1H), 3.29 (m, 1H), 3.20 (m, 1H), 2.45 (m, 1H), 2.16 (m, 1H), 1.80–1.59 (m, 2H), 1.44 (s, 9H), 1.44–1.41 (m, 2H), 1.02 (s, 9H), 1.01 (t, *J* = 9.4 Hz, 3H). HRMS calcd for C₄₅H₅₅N₅O₉S [M+H]⁺ 842.3799, found: 842.3814. HPLC purity (system 1: 96%, system 2: 96%). Compound **3c**: ¹H NMR (CD₃OD): δ 8.27 (d, *J* = 9.1 Hz, 1H), 7.80–7.74 (m, 2H), 7.51–7.44 (m, 5H), 7.40 (s, 1H), 7.28 (d, *J* = 8.2 Hz, 1H), 7.24 (dd, *J* = 2.5,

9.1 Hz, 1H), 6.61 (s, 1H), 6.41 (d, $J = 11.6$ Hz, 1H), 5.69 (s, 1H), 5.64 (m, 1H), 4.45 (t, $J = 7.4$ Hz, 1H), 4.00 (s, 3H), 3.84 (s, 1H), 3.50–3.12 (m, 2H), 2.45–2.17 (m, 2H), 1.96–1.70 (m, 4H), 1.47–1.41 (m, 2H), 1.44 (s, 9H), 1.03 (s, 9H), 0.97 (t, $J = 7.3$ Hz, 3H). HRMS calcd for $C_{45}H_{55}N_5O_9S$ $[M+H]^+$ 842.3799, found: 842.3780. HPLC purity (system 1: 89%, system 2: 90%). Compound **3d**: 1H NMR (CD_3OD (TFA salt), major isomer reported): δ 8.59 (d, $J = 9.3$ Hz, 1H), 7.87–7.80 (m, 2H), 7.74–7.53 (m, 6H), 7.37 (d, $J = 8.2$ Hz, 1H), 6.86 (s, 1H), 5.56 (s, 1H), 5.53 (m, 1H), 5.40 (ddd, $J = 6.2, 7.6, 15.2$ Hz, 1H), 4.46 (dd, $J = 6.7, 8.2$ Hz, 1H), 4.11 (s, 3H), 3.98 (s, 1H), 3.94 (dd, $J = 7.3, 15.0$ Hz, 1H), 3.83 (dd, $J = 6.5, 15.0$ Hz, 1H), 2.85 (m, 1H), 2.75 (m, 1H), 2.60 (m, 1H), 2.47 (m, 1H), 1.81–1.61 (m, 2H), 1.45–1.40 (m, 2H), 1.42 (s, 9H), 1.01 (s, 9H), 0.98 (t, $J = 7.4$ Hz, 3H). HRMS calcd for $C_{45}H_{55}N_5O_9S$ $[M+H]^+$ 842.3799, found: 842.3815. HPLC purity (system 1: 98%, system 2: 99%). Compound **3e**: 1H NMR (CD_3OD): δ 8.27 (d, $J = 9.2$ Hz, 1H), 7.87–7.84 (m, 2H), 7.66 (s, 1H), 7.56 (dd, $J = 2.3, 8.3$ Hz, 1H), 7.47 (d, $J = 2.6$ Hz, 1H), 7.49–7.40 (m, 3H), 7.27 (dd, $J = 2.5, 9.2$ Hz, 1H), 7.26 (d, $J = 8.3$ Hz, 1H), 6.69 (s, 1H), 6.55 (d, $J = 11.8$ Hz, 1H), 5.69 (m, 1H), 5.56 (s, 1H), 4.44 (t, $J = 7.6$ Hz, 1H), 4.02 (s, 1H), 4.00 (s, 3H), 3.27 (m, 1H), 3.14 (m, 1H), 2.90 (m, 1H), 2.47 (m, 1H), 1.82–1.61 (m, 2H), 1.52–1.35 (m, 2H), 1.43 (s, 9H), 1.02 (s, 9H), 0.99 (t, $J = 7.4$ Hz, 3H). HRMS calcd for $C_{44}H_{53}N_5O_9S$ $[M+H]^+$ 828.3642, found: 828.3668. HPLC purity (system 1: 97%, system 2: 63%). Compound **3f**: 1H NMR (CD_3OD (NH_4^+ salt)) δ 8.2 (d, $J = 9.2$ Hz, 1H), 7.78–7.75 (m, 2H), 7.50–7.45 (m, 5H), 7.32 (d, $J = 2.4$ Hz, 1H), 7.27 (dd, $J = 2.5, 9.2$ Hz, 1H), 7.24 (d, $J = 8.4$ Hz, 1H), 6.64 (s, 1H), 5.85 (ddd, $J = 5.9, 7.4, 15.4$ Hz, 1H), 5.75 (s, 1H), 5.51 (m, 1H), 4.55 (dd, $J = 6.9, 8.2$ Hz, 1H), 4.04 (s, 1H), 4.00 (s, 3H), 4.15–3.96 (m, 2H), 3.47–3.24 (m, 2H), 1.79 (m, 1H), 1.67 (m, 1H), 1.43 (s, 9H), 1.49–1.34 (m, 2H), 1.03 (s, 9H), 0.97 (t, $J = 7.3$ Hz, 3H). HRMS calcd for $C_{44}H_{53}N_5O_9S$ $[M+H]^+$ 828.3642, found: 828.3660. HPLC purity (system 1: 98%, system 2: 99%).

5.2.5. Compounds 4a, 4b and 4c

Starting material **4** was ring-closed using three different methods. *Method 1*: **4** (25.0 mg, 0.0300 mmol) and Grubbs 2nd catalyst (2.50 mg, 0.00300 mmol) were stirred in dry toluene (60 mL) in a round bottomed flask under N_2 -atmosphere and heated at 85 °C. The solvent was evaporated after 6 h of heating and the crude product was purified on silica (CH_2Cl_2 –MeOH 7%). *Method 2*: **4** (25.0 mg, 0.0300 mmol) and Grubbs 2nd catalyst (2.50 mg, 0.00300 mmol) were dissolved in dry trifluorotoluene (20 mL) in a microwave vessel. The vessel was sealed, evacuated and flushed with N_2 before heating by microwave irradiation at 110 °C for 5 min. The solvent was evaporated and the crude product was purified on silica (CH_2Cl_2 –MeOH 7%). *Method 3*: **4** (25.0 mg, 0.0300 mmol), Hoveyda-Grubbs 2nd catalyst (0.900 mg, 0.00150 mmol) and *p*-benzoquinone (0.320 mg, 0.00300 mmol) were dissolved in dichloroethane (20 mL) in a microwave vessel. The vessel was sealed, evacuated and flushed with N_2 before heating by microwave irradiation at 140 °C for 5 min. The solvent was evaporated and the crude product purified on silica (CH_2Cl_2 –MeOH 7%) before the outcomes of the methods were evaluated. The products obtained from using the different methods were combined (57.0 mg, 0.0770 mmol) and deprotected according to the general procedure. The resulting hydrochloride was mixed with Boc-L-tLeu (53.0 mg, 0.231 mmol), HATU (105 mg, 0.277 mmol) and DIEA (110 μ L, 0.631 mmol) in DMF (1.8 mL). After purification using preparative chiral HPLC (*i*-PrOH–*i*-hexane 30:70) followed by RP-HPLC (MeCN/ H_2O 0.05% HCOOH) or (MeCN/ H_2O with 25 mM NH_4OAc , pH 6.3), compounds **4a** (5.6 mg, 8.4%), **4b** (2.7 mg, 4.1%) and **4c** (1.7 mg, 2.5%) were isolated as white solids. Compound **4a**: 1H NMR (CD_3OD (NH_4^+ salt)) δ 8.33 (d, $J = 9.3$ Hz, 1H), 7.79–7.76 (m, 2H), 7.54 (d, $J = 2.4$ Hz, 1H), 7.50 (d, $J = 2.4$ Hz, 1H), 7.49–7.44 (m, 4H), 7.31 (dd, $J = 2.4, 9.0$ Hz, 1H), 7.21 (d, $J = 8.3$ Hz, 1H), 6.65 (s,

1H), 6.49 (d, $J = 15.7$ Hz, 1H), 6.29 (m, 1H), 5.75 (s, 1H), 4.60 (m, 1H), 4.02 (m, 1H), 4.01 (s, 3H), 2.25 (m, 1H), 2.15 (m, 1H), 1.92–1.81 (m, 2H), 1.79–1.58 (m, 4H), 1.55–1.38 (m, 4H), 1.43 (s, 9H), 1.02 (s, 9H), 0.97 (t, $J = 7.3$ Hz, 3H). ^{13}C NMR (CD_3OD) 174.2, 173.1, 172.4, 164.5, 164.0, 160.9, 157.8, 156.8, 151.2, 138.3, 136.6, 135.1, 132.7, 131.0, 130.5, 129.9, 128.8, 127.0, 125.3, 124.2, 123.2, 120.4, 115.8, 106.8, 102.0, 80.7, 63.7, 56.9, 56.3, 54.5, 53.9, 35.4, 35.1, 31.3, 28.8, 27.7, 27.2, 22.3, 20.2, 13.9. HRMS calcd for $C_{46}H_{57}N_5O_9S$ $[M+H]^+$ 856.3955, found: 856.3964. HPLC purity (system 1: 98%, system 2: 99%). Compound **4b**: 1H NMR (CD_3OD (NH_4^+ salt)) δ 8.30 (d, $J = 9.2$ Hz, 1H), 7.79–7.74 (m, 2H), 7.61 (m, 1H), 7.49 (d, $J = 2.5$ Hz, 1H), 7.48–7.42 (m, 3H), 7.39 (dd, $J = 2.3, 8.2$ Hz, 1H), 7.29 (dd, $J = 2.5, 9.2$ Hz, 1H), 7.22 (d, 8.3 Hz, 1H), 6.64 (s, 1H), 6.50 (d, $J = 15.8$ Hz, 1H), 6.45 (m, 1H), 5.51 (s, 1H), 4.74 (m, 1H), 4.01 (s, 3H), 3.88 (s, 1H), 3.74 (m, 1H), 3.28 (m, 1H), 2.28–2.08 (m, 2H), 1.94–1.73 (m, 4H), 1.72–1.55 (m, 2H), 1.50 (m, 1H), 1.43 (s, 9H), 1.30 (m, 1H), 1.02 (s, 9H), 0.97 (t, $J = 7.3$ Hz, 3H). ^{13}C NMR (CD_3OD (NH_4^+ salt)) δ 175.2, 173.8, 172.9, 164.0, 163.7, 161.0, 158.1, 152.5, 151.6, 140.7, 136.5, 134.9, 132.9, 131.3, 130.8, 129.9, 128.7, 127.9, 124.8, 124.0, 123.6, 120.2, 115.8, 107.5, 101.9, 80.8, 64.5, 59.1, 56.1, 54.4, 53.7, 35.7, 34.9, 30.7, 28.8, 28.3, 27.2, 22.4, 20.0, 14.0. HRMS calcd for $C_{46}H_{57}N_5O_9S$ $[M+H]^+$ 856.3955, found: 856.3964. HPLC purity (system 1: 95%, system 2: 97%). Compound **4c**: 1H NMR (CD_3OD (NH_4^+ salt)) δ 8.28 (d, $J = 9.4$ Hz, 1H), 7.84–7.79 (m, 2H), 7.65 (br s, 1H), 7.56 (dd, $J = 2.3, 8.3$ Hz, 1H), 7.52–7.40 (m, 4H), 7.30–7.25 (m, 2H), 6.60 (s, 1H), 6.34 (d, $J = 11.5$ Hz, 1H), 5.60–5.52 (m, 2H), 4.35 (dd, $J = 6.4, 8.7$ Hz, 1H), 4.01–3.98 (m, 4H), 2.19–2.10 (m, 3H), 1.91–1.79 (m, 1H), 1.77–1.63 (m, 3H), 1.60–1.47 (m, 3H), 1.43 (s, 9H), 1.29 (m, 1H), 1.18 (m, 1H), 1.00 (s, 9H), 0.99 (t, $J = 7.4$ Hz, 3H). ^{13}C NMR (CD_3OD (NH_4^+ salt)) δ 174.5, 172.9, 172.1, 164.4, 163.7, 160.5, 152.5, 152.0, 150.8, 140.0, 136.2, 135.8, 132.2, 131.1, 131.0, 130.2, 129.3, 128.5, 124.3, 124.1, 123.1, 120.1, 115.7, 107.1, 101.5, 80.7, 63.5, 57.4, 56.2, 55.0, 52.1, 35.5, 34.5, 28.9, 28.7, 27.5, 27.2, 24.6, 20.2, 13.9. HRMS calcd for $C_{46}H_{57}N_5O_9S$ $[M+H]^+$ 856.3955, found: 856.3943. HPLC purity (system 1: 97%, system 2: 99%).

5.2.6. Compound 4d

The combined products **4a** and **4c** (5.90 mg, 0.00689 mmol) were dissolved in MeOH (3 mL) and stirred together with PtO_2 (0.930 mg, 0.00413 mmol) in an H_2 -atmosphere until the starting material was no longer visible by LC–MS. The solution was filtered and evaporated. Purification by RP-HPLC (MeCN– H_2O (0.1% TFA)) yielded **4d** (0.8 mg, 13.5%). 1H NMR (CD_3OD (TFA salt)) δ 8.55 (d, $J = 8.7$ Hz, 1H), 7.82 (dd, $J = 7.8, 1.3$ Hz, 2H), 7.70–7.53 (m, 7H), 7.31 (d, $J = 8.7$ Hz, 1H), 6.86 (s, 1H), 5.62 (s, 1H), 4.43 (m, 1H), 4.10 (s, 3H), 4.02 (s, 1H), 3.08–2.93 (m, 2H), 1.84 (m, 1H), 1.77–1.67 (m, 2H), 1.61–1.46 (m, 5H), 1.42 (s, 9H), 1.36–1.28 (m, 3H), 1.16–1.08 (m, 3H), 1.01 (s, 9H), 0.98 (t, $J = 7.4$ Hz, 3H). HRMS calcd for $C_{46}H_{59}N_5O_9S$ $[M+H]^+$ 858.4033, found: 858.4118. HPLC purity (system 1: 95%, system 2: 99%).

5.3. Enzyme inhibition

The protease activity of the full-length HCV NS3 protein (protease–helicase/NTase) from genotype 1a was measured using a FRET-assay as previously described.^{36,43} In short, 1 nM enzyme was incubated for 10 min at 30 °C in 50 mM HEPES, pH 7.5, 10 mM DTT, 40% glycerol, 0.1% *n*-octyl- β -D-glucoside, 3.3% DMSO with 25 μ M of the peptide cofactor 2K-NS4A (KKGSVVIV-GRIVLSGK), and inhibitor. The reaction was started by the addition of 0.5 μ M substrate (Ac-DED(Edans)EEAbu Ψ [COO]ASK(Dabcyl)-NH₂) obtained from AnaSpec Inc. (San Jose, USA). Non-linear regression analysis of the data was made using Graft 5.0.13 (Erithacus software limited).

5.4. Computational methodology

All the ligands were built in maestro and geometry optimization is carried out using OPLS-2005 force field. The crystal structure of HCV bifunctional protease helicase (1CU1) is used in the study. This NS3 protein complex consists of the C-terminal helicase domain and the N-terminal protease domain with a covalently linked NS4A cofactor. The protease active site is occupied by the substrate (NS3 C-terminus which is part of the helicase domain). The active site was made available for the docking studies by deleting these terminal residues (624–631) occupying the active site.

All the crystallographic waters were removed and the protein was prepared for docking using the protein preparation tool implemented in the Schrödinger Suite 2008.⁴⁴ The generated structures were subjected to restrained minimization using the OPLS-2005 force field with 'normal' BatchMin cutoffs (7.0 Å VDW; 12.0 Å ELE). To account for the conformational changes in the protein, induced fit docking is carried out using FLO (also called QXP).⁴⁵ A truncated protein structure that included only amino acids within 9 Å from the residues 624–631 (C-terminus) was used in the docking studies using FLO. Protein flexibility is accounted for by allowing crucial amino acid residues in the binding pocket to move freely up to 0.2 Å. Movement larger than 0.2 Å was penalized by 20.0 kJ/mol/Å.² Flexible residues occupying the active site viz., R155, Q526 and K136 were given full conformational freedom. Constraints were applied to the inhibitor to restrict its translation away from the active site. For each inhibitor, 10 unique binding poses were generated using 2000 Monte Carlo perturbation cycles. These poses were further subjected to 20 steps of simulated annealing followed by energy minimization. Each cycle involves 400 rapid Monte Carlo steps generating unique conformations within an energy window of 50 kJ/mol/Å and an RMSD >0.5 Å. Each of the complexes was submitted to a 3 fs dynamics at 600 K after 3000 fs of equilibration steps. The maximum movement of an atom in any single step was limited to 0.1 Å. Hydrogen vibrations were damped by assigning an atomic weight of 10. Among the 10 best poses generated, the most plausible binding mode conformation for each compound was selected based on visual inspection.

Acknowledgments

We gratefully acknowledge support from Knut and Alice Wallenberg's foundation. We also thank Dr Aleh Yahorau, Department of Pharmaceutical Biosciences, Uppsala University, for help with HRMS analyzes and Medivir AB, Huddinge, Sweden for EC50-determinations and financial support.

References and notes

- Lavanchy, D. *Liver Int.* **2009**, 29, 74.
- Brown, R. S. *Nature* **2005**, 436, 973.
- Feld, J. J.; Hoofnagle, J. H. *Nature* **2005**, 436, 967.
- Takamizawa, A.; Mori, C.; Fuke, I.; Manabe, S.; Murakami, S.; Fujita, J.; Onishi, E.; Andoh, T.; Yoshida, I.; Okayama, H. *J. Virol.* **1991**, 65, 1105.
- Lindenbach, B. D.; Rice, C. M. *Nature* **2005**, 436, 933.
- Grakoui, A.; Wychowski, C.; Lin, C.; Feinstone, S. M.; Rice, C. M. *J. Virol.* **1993**, 67, 1385.
- Rosenberg, S. J. *Mol. Biol.* **2001**, 313, 451.
- Rönn, R.; Sandström, A. *Curr. Top. Med. Chem.* **2008**, 8, 533.
- Failla, C.; Tomei, L.; De Francesco, R. *J. Virol.* **1994**, 68, 3753.
- Gale, M.; Foy, E. M. *Nature* **2005**, 436, 939.
- Kolykhalov, A. A.; Mihalik, K.; Feinstone, S. M.; Rice, C. M. *J. Virol.* **2000**, 74, 2046.
- Lamarre, D.; Anderson, P. C.; Bailey, M.; Beaulieu, P.; Bolger, G.; Bonneau, P.; Bos, M.; Cameron, D. R.; Cartier, M.; Cordingley, M. G.; Faucher, A. M.; Goudreau, N.; Kawai, S. H.; Kukolj, G.; Lagace, L.; Laplante, S. R.; Narjes, H.; Poupard, M. A.; Rancourt, J.; Sentjens, R. E.; St George, R.; Simoneau, B.; Steinmann, G.; Thibeault, D.; Tsantrizos, Y. S.; Weldon, S. M.; Yong, C. L.; Llinas-Brunet, M. *Nature* **2003**, 426, 186.
- Llinas-Brunet, M.; Bailey, M.; Fazal, G.; Goulet, S.; Halmos, T.; Laplante, S.; Maurice, R.; Poirier, M.; Poupard, M. A.; Thibeault, D.; Wernic, D.; Lamarre, D. *Bioorg. Med. Chem. Lett.* **1998**, 8, 1713.
- Steinkühler, C.; Biasiol, G.; Brunetti, M.; Urbani, A.; Koch, U.; Cortese, R.; Pessi, A.; De Francesco, R. *Biochemistry* **1998**, 37, 8899.
- U. S. Food and Drug Administration <http://www.fda.gov/NewsEvents/Newsroom/PressAnnouncements/ucm255390.htm> (Accessed June 2011).
- Vertex Pharmaceuticals homepage: <http://www.vrtx.com/current-projects/approved-medicines/incivek.html> (Accessed June 2011).
- Ripka, A. S.; Rich, D. H. *Curr. Opin. Chem. Biol.* **1998**, 2, 441.
- Marshall, G. R. *Tetrahedron* **1993**, 49, 3547.
- Trabocchi, A.; Cini, N.; Menchi, G.; Guarna, A. *Tetrahedron Lett.* **2003**, 44, 3489.
- Jones, R. C. F.; Ward, G. J. *Tetrahedron Lett.* **1988**, 29, 3853.
- Marsault, E.; Peterson, M. L. *J. Med. Chem.* **2011**, 54, 1961.
- Vlieghe, P.; Lisowski, V.; Martinez, J.; Khrestchatsky, M. *Drug Discovery Today* **2010**, 15, 40.
- Venkatraman, S.; Njoroge, F. G. *Curr. Top. Med. Chem.* **2007**, 7, 1290.
- Tsantrizos, Y. S. *Biopolymers* **2004**, 76, 309.
- Condroski, K. R. Z. H.; Seiwert, S. D.; Ballard, J. A.; Bernat, B. A.; Brandhuber, B. J.; Andrews, S. W.; Josey, J. A.; Blatt, L. M. Structure-Based Design of Novel Isoindoline Inhibitors of HCV NS3/4A Protease and Binding Mode Analysis of ITMN-191 by X-ray Crystallography: *Digestive Disease Week*, May 20–25, Los Angeles, 2006, Poster #T1794.
- Mo, H. M.; Bae, A.; Sun, S. C.; Qi, X. P.; Chen, X. W.; Ku, K. R.; Worth, A.; Wong, K. A.; Harris, J.; Miller, M. D. *Antimicrob. Agents Chemother.* **2010**, 54, 5288.
- Raboisson, P.; de Kock, H.; Rosenquist, A.; Nilsson, M.; Salvador-Oden, L.; Lin, T.-I.; Roue, N.; Ivanov, V.; Wähling, H.; Wickström, K.; Hamelink, E.; Edlund, M.; Vrang, L.; Vendeville, S.; Van de Vreken, W.; McGowan, D.; Tahiri, A.; Hu, L.; Boutton, C.; Lenz, O.; Delouvroy, F.; Pille, G.; Surleraux, D.; Wigerinck, P.; Samuelsson, B.; Simmen, K. *Bioorg. Med. Chem. Lett.* **2008**, 18, 4853.
- Liverton, N. J.; Carroll, S. S.; DiMuzio, J.; Fandozzi, C.; Graham, D. J.; Hazuda, D.; Holloway, M. K.; Ludmerer, S. W.; McCauley, J. A.; McIntyre, C. J.; Olsen, D. B.; Rudd, M. T.; Stahlhut, M.; Vacca, J. P. *Antimicrob. Agents Chemother.* **2010**, 54, 305.
- McCauley, J. A.; McIntyre, C. J.; Rudd, M. T.; Nguyen, K. T.; Romano, J. J.; Butcher, J. W.; Gilbert, K. F.; Bush, K. J.; Holloway, M. K.; Swestock, J.; Wan, B. L.; Carroll, S. S.; DiMuzio, J. M.; Graham, D. J.; Ludmerer, S. W.; Mao, S. S.; Stahlhut, M. W.; Fandozzi, C. M.; Trainor, N.; Olsen, D. B.; Vacca, J. P.; Liverton, N. J. *J. Med. Chem.* **2010**, 53, 2443.
- Örtqvist, P.; Peterson, S. D.; Åkerblom, E.; Gossas, T.; Sabnis, Y. A.; Fransson, R.; Lindeberg, G.; Danielson, U. H.; Karlen, A.; Sandström, A. *Bioorg. Med. Chem.* **2007**, 15, 1448.
- Dahl, G.; Sandström, A.; Åkerblom, E.; Danielson, U. H. *Antivir. Ther.* **2007**, 12, 733.
- Örtqvist, P.; Vema, A.; Ehrenberg, A. E.; Dahl, G.; Rönn, R.; Åkerblom, E.; Karlen, A.; Danielson, U. H.; Sandström, A. *Antivir. Ther.* **2010**, 15, 841.
- Lampa, A.; Ehrenberg Angelica, E.; Gustafsson Sofia, S.; Vema, A.; Åkerblom, E.; Lindeberg, G.; Karlen, A.; Danielson, U. H.; Sandström, A. *Bioorg. Med. Chem.* **2010**, 18, 5413.
- Wang, A. X.; Scola, P. M. *WO* 2010/077783, 2010.
- Hong, S. H.; Sanders, D. P.; Lee, C. W.; Grubbs, R. H. *J. Am. Chem. Soc.* **2005**, 127, 17160.
- Poliakov, A.; Hubatsch, I.; Shuman, C. F.; Stenberg, G.; Danielson, U. H. *Protein Expr. Purif.* **2002**, 25, 363.
- Lohmann, V.; Korner, F.; Koch, J. O.; Herian, U.; Theilmann, L.; Bartenschlager, R. *Science* **1999**, 285, 110.
- Courchay, F. C.; Sworen, J. C.; Ghiviriga, I.; Abboud, K. A.; Wagener, K. B. *Organometallics* **2006**, 25, 6074.
- Schmidt, B. *Eur. J. Org. Chem.* **2003**, 816.
- Fuerstner, A.; Thiel, O. R.; Ackermann, L.; Schanz, H.-J.; Nolan, S. P. *J. Org. Chem.* **2000**, 65, 2204.
- Feldman, J.; Murdzek, J. S.; Davis, W. M.; Schrock, R. R. *Organometallics* **1989**, 8, 2260.
- Fu, G. C.; Grubbs, R. H. *J. Am. Chem. Soc.* **1992**, 114, 7324.
- Johansson, A.; Poliakov, A.; Åkerblom, E.; Lindeberg, G.; Winiwarter, S.; Samuelsson, B.; Danielson, U. H.; Hallberg, A. *Bioorg. Med. Chem.* **2002**, 10, 3915.
- Maestro v.8.5; Schrödinger Inc.: 101 SW Main Street, Suite 1300, Portland, OR, 97204.
- McMartin, C.; Bohacek, R. S. *J. Comput. Aided Mol. Des.* **1997**, 11, 333.